Mon. Not. R. astr. Soc. (1990) **243**, 480–491

New SiO masers associated with bright southern *IRAS* sources

P. J. Hall ★
School of Electrical Engineering, University of Sydney, NSW 2006, Australia

David A. Allen
Anglo-Australian Observatory, PO Box 296, Epping, NSW 2121, Australia

Euan R. Troup, R. M. Wark and Alan E. Wright
Australia Telescope National Facility†, PO Box 76, Epping, NSW 2121, Australia

Accepted 1989 October 11. Received 1989 October 10; in original form 1989 July 20

SUMMARY

We report the discovery of 31 new SiO $v=1$, $J=1-0$ (43.122 GHz) masers associated with southern *IRAS* sources. The candidate list for our search was produced systematically and the high detection success rate (~ 50 per cent) leads us to consider differences between stars associated with masers and those showing no maser emission.

We propose a set of conditions which virtually guarantee the presence of a detectable stellar SiO maser. One of the most important requirements is large optical variability (≥ 2.5 mag): a condition which we associate with high mass-loss rate. In addition, we find that the maser-to-infrared flux ratio is approximately proportional to the mass-loss rate.

New polarization observations of the SiO maser associated with R Aqr, one of the two symbiotic stars known to show any type of maser emission, are also presented. These are compared with our earlier records and, on the basis of an observed position angle similarity, it is suggested that the polarization mechanism is driven by the stellar magnetic field.

1 INTRODUCTION

More than 15 years have passed since the first observations of SiO masers associated with late-type stars. Notwithstanding significant observational and theoretical advances, the nature of the emission is still only poorly understood. The source of the population inversion remains in doubt and important characteristics of the radiation, such as secular intensity changes and curious polarization properties, remain unexplained. Undoubtedly, the lack of a large and homogeneous data set suitable for statistical studies is a contributing factor to the uncertainties. We present here results of new southern hemisphere observations which expand significantly the existing SiO database and which form, in themselves, a uniform data set compiled on the basis of stellar infrared attributes.

In an earlier paper (Allen *et al.* 1989; hereafter Paper I) we reported the discovery of 12 SiO $v=1$, $J=1-0$ (43.122 GHz) masers, including one associated with a symbiotic star. This previous work identified several Mira-like stars with unusually low maser/infrared flux density ratios and pointed to the need to examine the accepted correlation between maser and infrared (IR) emission levels. For the present study we therefore prepared an observing programme in which stars were selected according to their 12 μm flux; this allowed us to examine the maser–IR flux correlation and to explore statistically the maser-to-IR flux ratio, a distance-independent parameter which we suspected was related to stellar classification.

The candidate list for the present observations was drawn from the *IRAS Point Source Catalog* with the following selection criteria being applied (S_x is the catalogued flux density at x μm):

(i) declination south of $+10°$;
(ii) $S_{12} \geq 100$ Jy;
(iii) $S_{12}/S_{25} > 1$.

Criterion (iii) was introduced to give some rejection of non-stellar objects, but in retrospect it could have been relaxed

★ Present address: Australia Telescope National Facility†, PO Box 76, Epping, NSW 2121, Australia.
†The Australia Telescope National Facility is operated in association with the Division of Radiophysics by CSIRO.

since some SiO maser sources proved to have $S_{12} \sim S_{25}$. We excluded the following types of object from the list:

(i) bright and late-type stars with no record of variability;
(ii) class I supergiants;
(iii) known RV Tauri stars;
(iv) C and S stars (classified from either optical or *IRAS* low-resolution spectra);
(v) emission line stars such as B[e] types;
(vi) dark globules and reflection nebulae.

Using these selection and exclusion criteria, a final list of 182 sources was produced; 38 of these objects were known SiO masers. Due to telescope scheduling constraints we were unable to examine all the remaining sources. The sample of 60 candidates chosen for observation consists of bright objects at 12 μm which had not been associated previously with SiO maser emission. These 60 objects are distributed fairly uniformly in right ascension, with the result that the Galactic Bulge (where up to one-third of the sources in our final list are located) is under-represented in the sample. Also, to maximize the likelihood of obtaining optical and other data, the sample was chosen to have a preponderance of optically identified objects. Thirty-one new SiO masers were detected, giving a detection rate of ~50 per cent. Finally, in view of the brightness of some carbon stars at 12 μm and the existence of O-rich envelopes in some (Willems & de Jong 1986), supplementary observations were made of ten C stars; none proved detectable as SiO masers.

Paper I also examined the SiO maser emission from the symbiotic star R Aqr and, using published observations taken over a 10-yr period, placed constraints on the orbital dynamics of the masing component. New observations of R Aqr show emission velocity limits within the range apparent in our earlier investigation. Despite significant profile changes, the position angles of some linearly polarized features in the 1987 and 1988 spectra are remarkably similar. We suggest that, in the case of R Aqr, a polarization model involving the relatively stable stellar magnetic field may be more appropriate than the model proposed by Western & Watson (1983, 1984). Their model invokes asymmetries in the geometry of the generating region to explain linear polarization in SiO masers.

2 OBSERVATIONS

Observations were made at Parkes during the period 1988 August 25–30. At 43 GHz the inner 16.7 m of the 64 m paraboloid forms the reflecting surface; previous measurements (Hall, Wark & Wright 1987) give the antenna beamwidth as 1.6 arcmin, the aperture efficiency as 34 per cent and the sensitivity as 39 Jy K^{-1}.

The receiver used was a maser superheterodyne type tuned to give a single-sideband power response centred on the 43.122 GHz $v=1$, $J=1-0$ SiO maser transition. A wideband horn feed sensitive to one linear polarization is an integral part of this receiver assembly. The instantaneous bandwidth of the receiver is approximately 100 MHz and is limited mainly by the maser amplifier. In operation, the whole receiving package mounts on a rotatable platform at the telescope prime focus.

A system equivalent noise temperature of 130 ± 10 K was measured using the hot–cold load method in which ambient and liquid nitrogen temperature absorbers are placed alternately in front of the feed. During this test the equivalent temperature of a switchable noise calibration signal (injected after the feed) was also determined. Throughout the observing session the calibration signal was used as the basis for system monitoring; noise temperatures in the range 120–180 K were common.

The 300 MHz IF output of the receiver was converted to baseband, then passed to the Parkes one-bit autocorrelation spectrometer. Due to a hardware fault, only 768 of the 1024 spectrometer channels were usable. With 1 MHz overlap between three adjacent 10 MHz (256 channel) bands, a coverage of 28 MHz was obtained, corresponding to a velocity search range of 195 km s^{-1}. The raw velocity resolution was 0.27 km s^{-1} but spectra were Hanning smoothed during processing, resulting in a final resolution of 0.45 km s^{-1}.

Each candidate object was observed using alternating source–reference telescope positions (Paper I), resulting in quite flat spectral baselines. Candidate stars were usually observed for 30 min (15 min on-source time) giving an rms noise level ~2 Jy. Longer integrations were often taken on objects detected successfully.

Telescope pointing was checked using continuum sources and known SiO masers. When masers were used, the matched filter method described in Paper I was employed. Residual pointing errors were about 12 arcsec (rms) in both coordinates and the pointing solution obtained using a multiparameter fit remained stable during the period of observation.

The injected noise signal was used as a flux density calibration reference, the noise generator output itself being calibrated against several unpolarized continuum sources and checked independently during the hot–cold load tests. The error in flux density determination is estimated to be less than ± 20 per cent. A first-order correction for atmospheric attenuation has been applied to measured flux densities. An attenuation function of the form $e^{\tau \sec(Z)}$ was assumed, where Z is the telescope zenith angle and τ, the attenuation at $Z=0$, was taken as 0.1 (Balister *et al.* 1977).

Most spectra were recorded at arbitrary position angles but, when polarization measurements were made, the rotatable platform carrying the receiver and feed assembly was re-positioned continuously under computer control, ensuring that the selected feed position angle (PA) on the sky was maintained to an accuracy of $\pm 0.5°$. Spectra for three Stokes parameters were computed using the relationships

$$I_j = S_j(0) + S_j(90)$$

$$Q_j = S_j(0) - S_j(90)$$

$$U_j = S_j(45) - S_j(135),$$

where $S_j(\Phi)$ is the flux density in spectrometer channel j at PA$=\Phi$ degrees. The linear polarization, L, and source position angle, χ, are then given by

$$L_j = (Q_j^2 + U_j^2)^{1/2}$$

$$\chi_j = 1/2 \arctan(U_j/Q_j).$$

The noise probability density function in the linear polarization vector L is non-Gaussian, and to compensate for the

systematic positive bias we use a correction of the form

$$L_j = L_j'[1-(\sigma/L_j')^2]^{1/2},$$

where L_j' is the uncorrected linear polarization and σ is the larger of the rms noise levels in the U and Q spectra (Wardle & Kronberg 1974; Barvainis & Predmore 1985).

To minimize the effect of feed position errors, spectra taken at platform position angles separated by 180° were averaged prior to computation of the Stokes parameters. Tests on unpolarized sources showed residual polarization effects to be no greater than 3 per cent.

3 RESULTS

The new masers are listed in Table 1 and the corresponding emission profiles for all sources except GL5552 are presented in Fig. 1. In general, the signal–reference position alternation mentioned in the previous section was effective in producing baselines with minimal residual curvature. The residual was removed by fitting a linear or quadratic baseline to regions of the spectrum outside the maser lines, then subtracting the fitted baseline prior to plotting. In all cases radial velocities are relative to the local standard of rest (lsr). Spectra shown in Fig. 1 were recorded at arbitrary position angles, and flux density scales therefore assume no source polarization.

Table 2 is a list of non-detections; the sensitivity is set at $3\sigma_c$, where σ_c is the rms noise level in collated but unsmoothed spectra for the candidate object. The velocity search range for all objects was -97 to $+97$ km s^{-1}. In all but one case, sources classified as spectral type C are stars identified as carbon-rich on the basis of LRS records (*IRAS* Science Team 1986); we include in this category stars with LRS spectra similar to *IRAS* 15194−5115 (Meadows, Good & Wolstencroft 1987). The exception is GL 865, a carbon star (Merrill & Stein 1976) having an O-rich spectrum in the LRS band (*cf.* Willems & de Jong 1986).

Where ephemerides were available, an optical phase at the time of observation, expressed in fractional cycles from maximum light, has been included in Tables 1 and 2. Phases have been calculated using data from the *General Catalog of Variable Stars* (Kholopov 1985). Long-term studies of $v=1$, $J=2-1$ (86.243 GHz) SiO maser emission show good correlation between optical and SiO cyclic intensity changes, with large SiO intensity variations reported in some objects (Nyman & Olofsson 1986). Further observation of our non-detections may therefore be worthwhile, especially if the optical phase at the time of observation was in the range 0.4–0.8.

Haikala (1989) has recently reported the detection of $v=1$, $J=2-1$ SiO maser emission in three of the sources listed in Table 1: U Dor, RW Vel and GL5552. He also detected emission in this transition from CM Vel and V342 Sgr, two sources not detected in the present survey.

Fig. 2 shows polarization spectra for GL5552, the strongest of the new masers. The total intensity (I), linear polarization (L), fractional polarization (L/I) and position angle (χ) are plotted. For this source, the peak and integrated fluxes listed in Table 1 relate to the total intensity. The fractional polarization does not exceed 0.3 (the profile average is 0.084) and the form of the position angle variation is rather similar to the 1988 R Aqr profile shown in Fig. 3(a). Fig. 3(b) shows R Aqr spectra formed from our 1987 (Paper I) data.

Both R Aqr data sets were taken at essentially the same optical phase and the integrated total flux density is quite

Table 1. Successful detections.

IRAS Source	Other Name	Spectral Type	Period (Day)	Optical Phase	Peak Flux Density (Jy)	Integrated Flux Density (Jy km s^{-1})
00193-4033					28	173
02351-2711	IRC-30023	M9			17	137
05052-8420	SVS 1835				44	281
05096-4834	S Pic	M6-8e	428	0.2	25	69
05098-6422	U Dor	M5	394	0.5	125	424
07021-0852	HN Mon	M8	410	0.7	21	90
07152-3444	GL 1099	M6-7			29	183
07329-2352	DU Pup	M	550	0.4	76	258
09185-4918	RW Vel	M7e	433	0.9	62	200
09235-2347	IRC-20188	M9			14	78
10323-4611					11	67
11466-4128	X Cen	M5-6e	315	0.1	6	20
13442-6109	GL 4178				43	354
14020-3515	AQ Cen	Me	388	0.6	12	49
15099-5509					28	60
15287-5811					12	114
15502-5424	OH 327.4-0.6				19	53
15568-4513					16	58
16292-5004					5	18
16340-4634					17	89
16438-1133	V446 Oph	M8	341	0.2	20	158
17328-3327					8	12
17501-2656	OH 2.6-0.4	M8-9			35	266
17513-2313	V774 Sgr	M5			12	55
17570-3713	EK CrA		435	0.1	19	67
18135-1641	IRC-20454	M7			26	217
18280-5639	SS Tel		415	0.8	7	58
18387-0423	IRC 00363	M0			77	592
18595-3947	GL 5552	M			362	2140
20075-6005	X Pav	Mc	199		27	131
23213-4521	SVS 14540				32	155

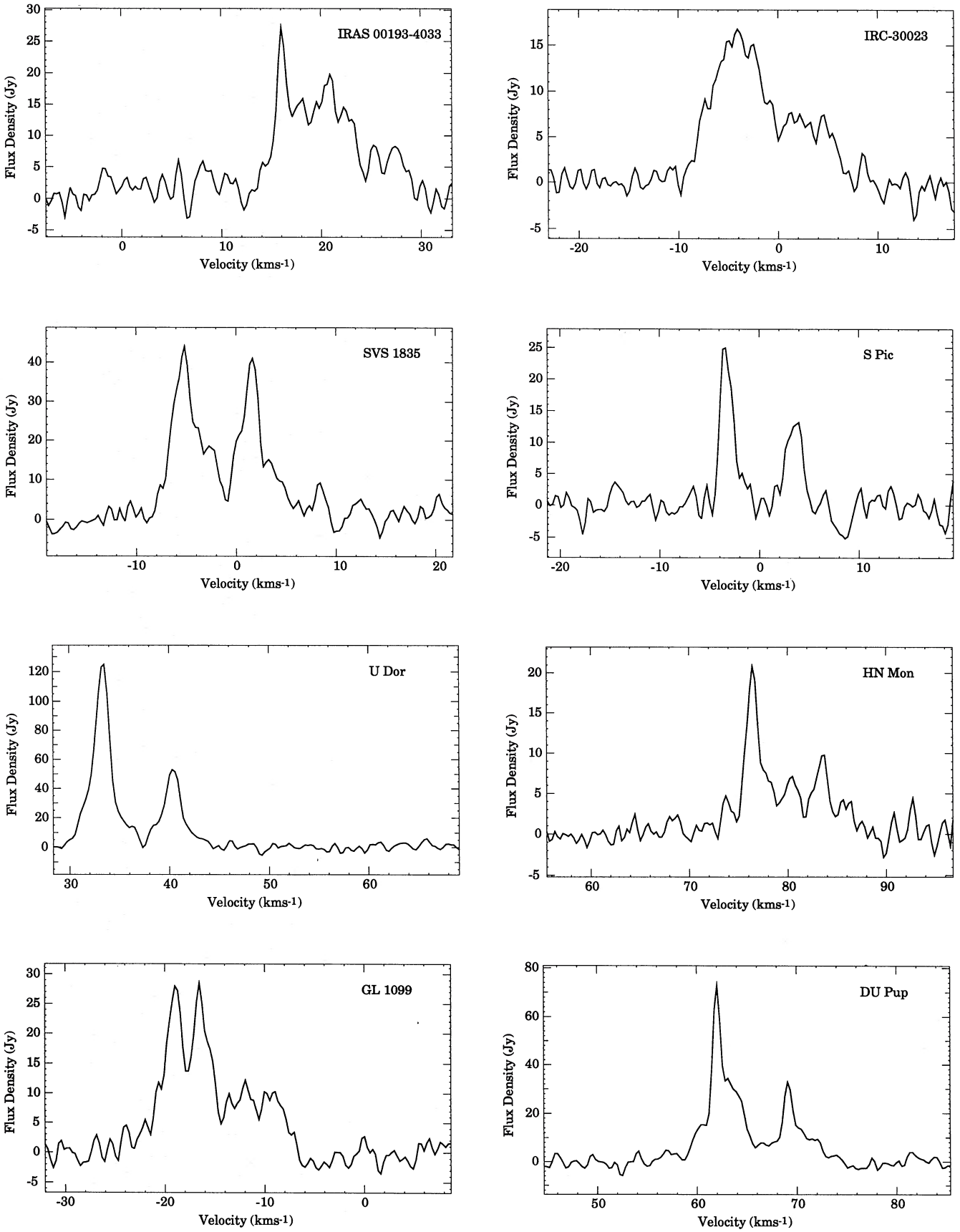

Figure 1. Emission profiles for 30 of the 31 new $v=1$, $J=1-0$ SiO masers arranged in the order listed in Table 1. Profiles for GL5552 are shown separately in Fig. 2. Velocities are relative to the local standard of rest (lsr) and all observations were made in the period 1988 August 25–30. Spectra were taken at arbitrary position angles, and flux density scales therefore assume no maser polarization.

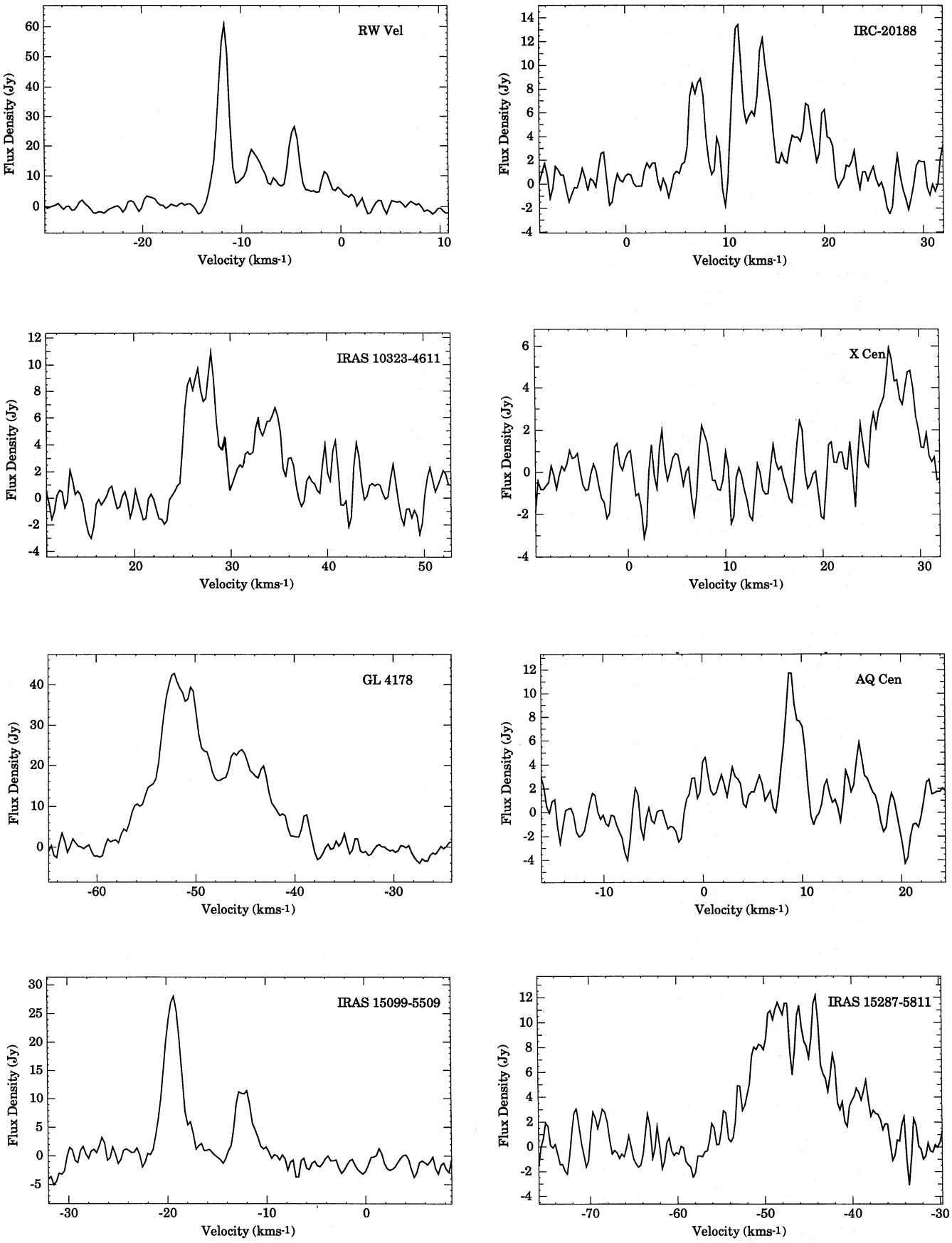

Figure 1 – *continued*

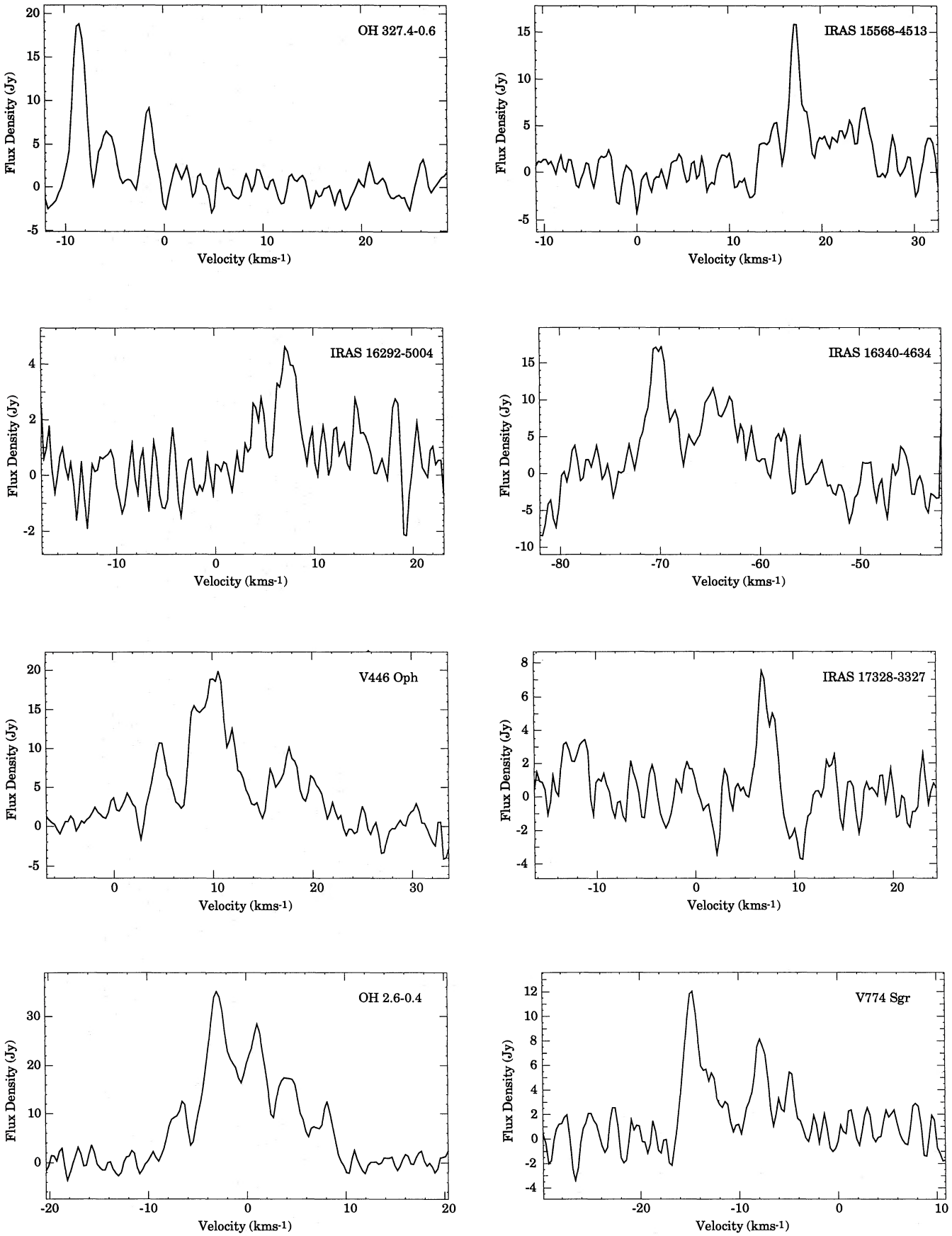

Figure 1 – *continued*

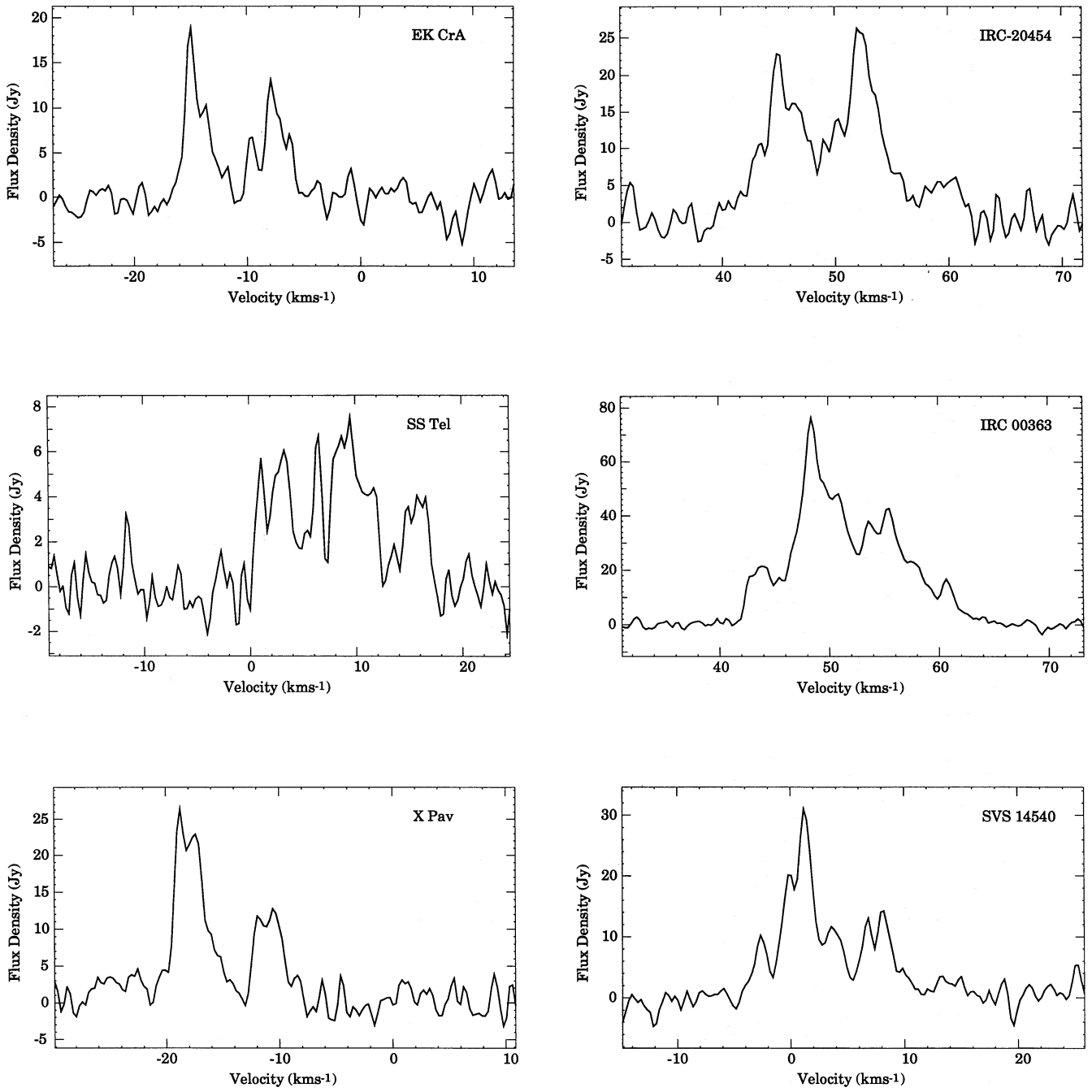

Figure 1 – *continued*

similar (1097 Jy km s^{-1} in 1988; 823 Jy km s^{-1} in 1987). However, the 1988 peak intensity is reduced to almost one-third of that recorded in the earlier study. The profile has also changed considerably, but the velocity range of the emission is contained between the -37 and -17 km s^{-1} limits established in Paper I. The new observations therefore yield no further information about the dynamics of the masing regions.

The fractional linear polarization differs from feature to feature in both data sets but the highest fractional polarization in 1988 is 0.45, compared with almost complete polarization for some minor features in the earlier profile. The profile-averaged fractional polarization values in 1988 and 1987 are 0.20 and 0.41, respectively. Variations in profile make it difficult to relate individual features in the two data sets but, where regions of significant, polarized emission coincide in the body of the profiles, the position angles are quite similar.

Table 2. Upper limits for undetected sources.

IRAS Source	Other Name	Spectral Type	Period (Day)	Optical Phase	Sensitivity (Jy)
00245-0652	UY Cet	M7	440	0.9	7.3
02427-5430	W Hor	Mc	137		7.6
04382-1417	BX Eri	M2-7	165	0.2	5.7
05592-0221	V352 Ori	M7			6.5
06036-2411	S Lep	M6	89		6.7
08220-0821	FK Hya	M6			8.8
08375-1707	AK Hya	M4	75?		7.0
10056-5300	CM Vel	M8.5	780	0.9	9.8
10580-1803	R Crt	M7	160		7.2
12230-5943	ST Cru	M6e	440	0.0	7.9
12233-5920	GL 4845S				9.8
12277+0441	BK Vir	M7	150		8.4
12319-6728	BO Mus	M6			8.2
13114-0232	SW Vir	M7	150		8.4
14086-0730	OH 334.7+50.0	M7			6.0
14280-2952	Y Cen	M4-7e	180		7.0
15214-2244	RS Lib	M7-8	218		8.0
17187-3750					7.0
18455-0200	AB Aql	M6			7.7
18513+0035	IRC 00389				11.2
18560-2954	V3953 Sgr	M9			10.0
19093-3256	V342 Sgr	M9	372	0.9	7.0
19143-5032	V Tel	M6-8	125		8.4
21044-1637	RS Cap	M4	149	0.4	9.6
21069-3843	GL 5592				7.0
21243-6943	SX Pav	M5-7	50		8.9
22230-4841	S Gru	M5-8e	307	0.6	8.0
22525-2952	V PsA	Mb	148		7.2
23063-3024	Y Scl	M4			6.0
06012+0726	GL 865	C			7.3
09116-2439	GL 5254	C			7.4
09521-7508	GL 4098	C			8.2
12540-6845		C			10.4
13477-6532	GL 4183	C			9.4
14484-6152		C			7.2
15082-4808	GL 4211	C			7.2
15194-5115		C			7.1
17049-2440	GL 1922	C			6.0
18194-2708	GL 2135	C			6.6

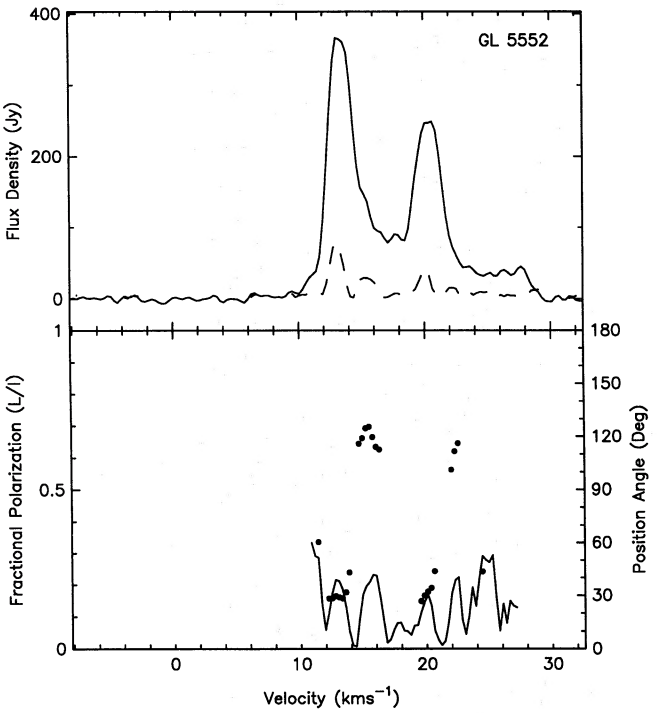

Figure 2. Polarization spectra for GL5552, the strongest of the new masers, recorded 1988 August 26. The upper panel shows the Stokes parameter, I (solid line), and the linearly polarized flux, L (broken line); the lower panel shows the fractional polarization, L/I (solid line), and the position angle, χ (dots). Polarized flux, fractional polarization and position angle are plotted over the range where the formal error in position angle is less than $\pm 15°$.

4 DISCUSSION

4.1 Radio–IR fluxes and optical variability in masers

We have examined our detections and non-detections in a search for differences between the two groups. The mean IR flux at 12, 25 and 60 μm is higher on the average for masers than for non-masers, but the differences are not significant statistically. However, the spectral index between 12 and 25 μm is significantly lower for sources which we detect as masers than for those not detected (i.e. the sources showing maser emission are redder). When the S_{25}/S_{60} ratio is considered, the two groups are indistinguishable.

This difference in mean S_{12}/S_{25} for the two groups is attributed to an observational selection effect. Our 12 μm flux density criterion for choosing candidates discriminates against bluer objects and, furthermore, the Parkes candidate list did not include known SiO masers, many of which had been selected previously for observation on the basis of their optical (rather than IR) properties. The sample of candidates observed by us therefore contains a large number of redder objects. No significant difference in spectral index between masers and non-masers is observed if we consider all previous surveys as well as the present one.

In Paper I we demonstrated a correlation between peak 43.122-GHz SiO maser flux density and mean 12 μm *IRAS* flux density. The new sources listed in Table 1 fall within the earlier scatter limits, neither improving nor degrading the correlation. We use peak maser fluxes in correlation analyses to allow useful upper limits to be given, but our SiO–IR flux correlation is not improved significantly if integrated SiO fluxes are used. However, Bujarrabal, Planesas & del

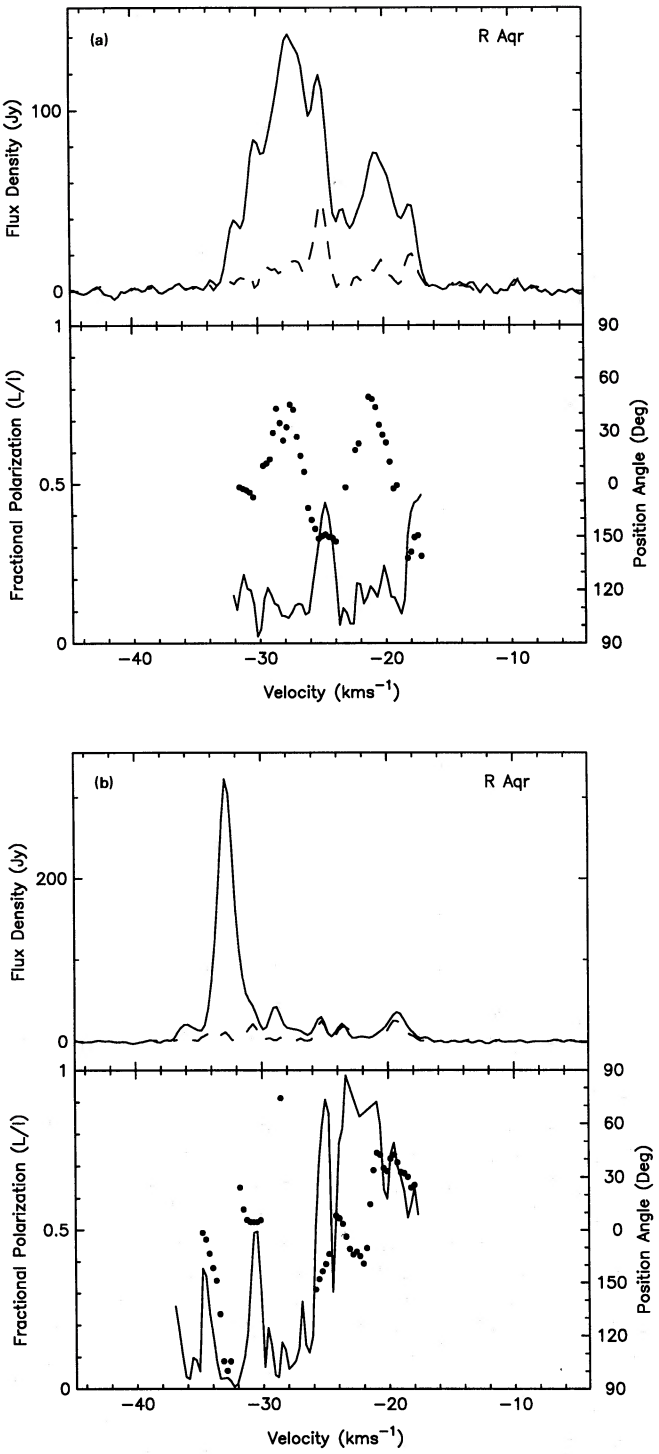

Figure 3. Spectra for the R Aqr maser recorded (a) in 1988 August 29 and (b) in 1987 July 30. The upper panel in each case shows I (solid line) and L (broken line). The lower panel shows L/I (solid line) and χ (dots). The definitions and plot ranges for L, L/I and χ are as for Fig. 2.

Romero (1987) find that the use of distance-corrected integrated flux data taken at constant optical phase results in better correlation. Although the correlation is evident at several IR wavebands, they find the best overall result at 8 μm, the wavelength of the $v=1-0$ SiO vibrational transition. They argue that the observed linear proportionality is an expected property of a radiatively pumped saturated maser.

The correlation between SiO maser peak intensity and *IRAS* 12 μm flux exhibits quite large scatter, greatly exceeding the observational uncertainties. Even ignoring the symbiotic stars, most of which appear to be underluminous in all maser emission, the flux ratio [SiO]/S_{12} has an rms scatter of about 0.3 dex, or a total spread in the samples approaching two orders of magnitude. The larger sample we now have allows us to explore the scatter in greater detail and, in particular, to seek a second parameter (other than source secular variability) which might explain the spread. In a radiative pumping model the distance–independent ratio [SiO]/S_{12} is a measure of the conversion efficiency between IR and maser emission; in our study it is defined as the highest recorded peak flux density of the maser emission to the *IRAS* 12 μm flux density, both expressed in jansky.

For a more complete analysis we have supplemented our own data with all published 43.122 GHz observations of objects in the northern hemisphere which otherwise satisfy the criteria described in Section 1. The resulting data set contains over 140 *IRAS* sources and includes successfully detected SiO masers as well as non-detections. Published optical data are available for about 70 of the sources, and for these objects we have explored the dependence of [SiO]/S_{12} on several stellar parameters. No convincing correlation with spectral type or IR colour was found, but there is a weak dependence on variable type, with semi-regular variables yielding generally smaller [SiO]/S_{12} ratios than Miras. The relationship becomes more striking when the parameter is quantified in terms of the range of optical variation: stars having large ranges have larger [SiO]/S_{12} values.

This trend is illustrated in Fig. 4, a plot of [SiO]/S_{12} against visual amplitude (or, where necessary, a representative visual amplitude derived from data at other wavelengths). Fig. 4 demonstrates that *IRAS* sources identified with late-type stars having amplitudes >2.5 mag are very frequently detected as SiO masers. Furthermore, a correlation between amplitude and [SiO]/S_{12} is apparent, with the dependence of [SiO]/S_{12} probably being even steeper than it appears, since only the most intense SiO masers have been detected at small visual ranges. Approximately one decade in [SiO]/S_{12} scatter is accounted for by this correlation: at any given visual amplitude the scatter has been reduced to little more than one order of magnitude total spread, or an rms of 0.15 dex. No further reduction of the scatter is apparent if integrated rather than peak SiO fluxes are used.

The SiO maser emission from most stars has been sampled only once or twice, and there is abundant evidence that the emission from some sources exhibits large intensity variations. The variation is correlated with optical phase (e.g. Bujarrabal, Planesas & del Romero 1987), although our R Aqr data (Fig. 3) and the study by Nyman & Olofsson (1986) show that cycle-to-cycle variations also occur. We suspect that secular flux density variations of individual stars now dominate the scatter in Fig. 4, and that considerably more observational coverage is needed for significant improvement.

Nonetheless, two stars lying to the lower right in the plot can be identified as discrepant. One, R Cen, was noted to be an underluminous (undetected) maser in Paper I. It is a class II supergiant and may indicate that these stars, like the class I

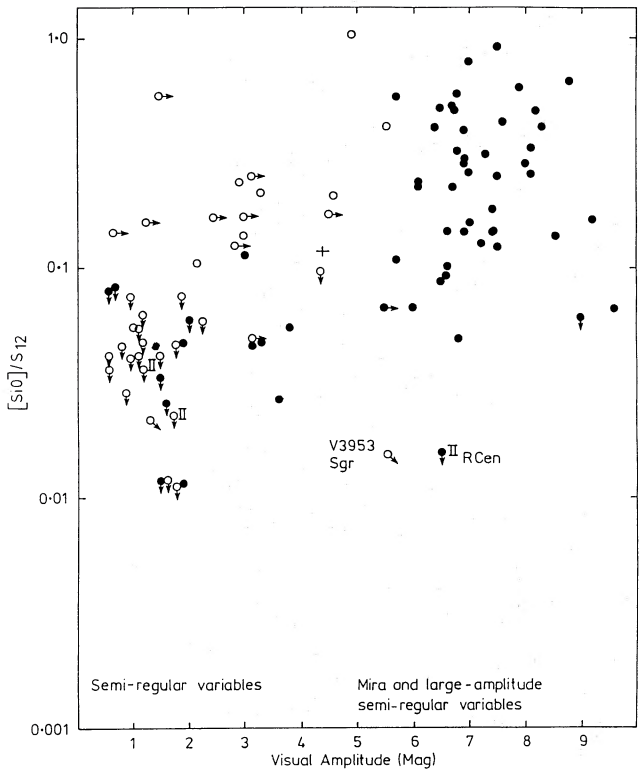

Figure 4. Plot of the $[SiO]/S_{12}$ ratio as a function of the visual amplitude listed in the *General Catalog of Variable Stars* (Kholopov 1985). When V magnitudes were unavailable, scaled photographic or I-band magnitudes were used to derive representative values. Photographic magnitudes were multiplied by 0.75; I-band data were doubled. Points derived by scaling are indicated by open circles (denoting photographic data) or crosses (I-band). Points labelled 'II' represent class II giants. The most interesting discrepant points are identified. Notice that stars having visual amplitudes in excess of 2.5 mag are almost invariably detected as 43.122-GHz SiO masers.

supergiants, do not obey the same relationships as the class III giants. The upper limits on the other two class II stars in our sample (V Eri and CM Vel) are too high to strengthen this suggestion. Alternatively, R Cen may in fact be a large-amplitude SiO maser observed coincidentally at a flux minimum. The other discrepant star, V3953 Sgr, is little-known, although a spectral type of M9 is given by Kholopov (1985). Further study of this star is needed to explain its non-conformism, for example by showing it to be an S star.

The sample of 70 detected and potential masers used to produced Fig. 4 was selected on the basis of a 100 Jy lower limit in IR flux density. With radio detection sensitivity limits of 1–10 Jy for our own and some other observations, upper limits for $[SiO]/S_{12}$ in the range 0.01–0.1 are obtained. This range is evidently sufficiently low to divide clearly the maser and non-maser populations on the basis of visual amplitude. However, it is important to examine selection effects which may influence the interpretation of Fig. 4. In particular, the scarcity of sources in the lower right and upper left of the diagram needs consideration.

Sources likely to fall in the lower right region are well-studied, large-amplitude stars of the type which form the traditional search base for SiO masers. It is likely therefore that the paucity of sources in this region is a real effect. The few maser sources in the upper left of Fig. 4 are mainly faint (and probably highly reddened) objects whose variabilities have been determined photographically. Since their apparent luminosities at minimum light fall below the limits of present photographic surveys, their true visual amplitudes may be considerably greater than the lower limits plotted, strengthening the association between SiO maser activity and relatively large visual range. The use of IR selection criteria has enabled us to examine this upper left region of the diagram more effectively than would be possible with optical criteria. While we cannot exclude the possibility of a new population of objects which have associated SiO masers, weak variability, and high extinction (e.g. by circumstellar dust shells), the simplest explanation is that objects falling in this region of Fig. 4 are simply large-amplitude, highly reddened Miras.

What is the meaning of the correlation between the ratio $[SiO]/S_{12}$ and variability range? First, we must consider the significance of the visual amplitude. This parameter is related to several physical variables, including the surface temperature (and hence spectral type) of the star. In the main, however, it may be regarded as a rough measure of mass-loss rate: stars with large visual amplitudes are almost certainly those losing mass most rapidly. To support this contention we present (Fig. 5) a plot of mass-loss rate versus visual amplitude for 38 M-giants examined by Gehrz & Woolf (1971). The mass-loss rates derived by them are based on measurement of the optical depth of 10 μm silicate features. According to Bowers (1985), derivations from IR data agree reasonably well with more recent CO-based estimates for stars where both types of determination are available. Fig. 5 shows that, over the visual range plotted in Fig. 4, the relationship between mass-loss rate and amplitude is

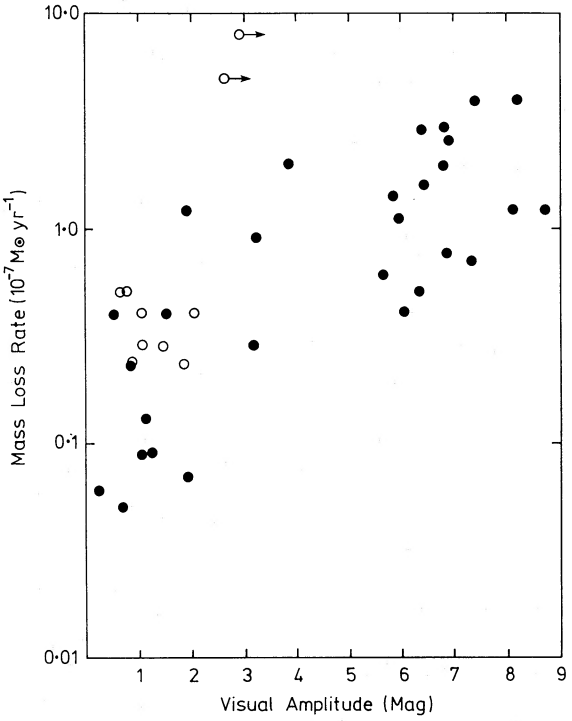

Figure 5. Plot of mass-loss rate as a function of magnitude of optical variation for 38 M-giant stars (Gehrz & Woolf 1971). Open circles represent stars for which the visual amplitude has been estimated by multiplying the photographic amplitude by 0.75.

approximately linear. We therefore regard the abscissa of Fig. 4 as a roughly linear representation of mass-loss rate and conclude that $[SiO]/S_{12}$ is approximately proportional to mass-loss rate.

In a few cases (<10), CO-based mass-loss data are available for stars plotted in Fig. 4 (Knapp & Morris 1985). When $[SiO]/S_{12}$ is plotted as a function of these mass-loss rates, there is considerable scatter but the suggested correlation is not destroyed. Mass-loss data pertaining specifically to the objects considered in Fig. 4 would clearly be invaluable in examining further the suggested relationship.

Bowers (1985) summarized earlier investigations of a putative dependence of maser luminosity on mass-loss rate. He presented a well-defined dependence for OH and H_2O masers, a conclusion supported for the OH sources by the recent work of Sivagnanam *et al.* (1989). However, the 12 SiO masers considered by Bowers show only a weak dependence, and he cited references suggesting that, for these sources, the maser luminosity may depend more strongly on the bolometric luminosity than on mass-loss rate. Since we do not attempt to ascribe distances to sources, our study cannot directly relate maser luminosity to mass-loss rate. Rather, Fig. 4 demonstrates the importance of mass-loss rate in determining whether SiO maser action occurs. Since classical Miras have large visual amplitudes, our data support the suggestion (e.g. Dickinson *et al.* 1978) that all O-rich Mira stars are SiO masers: successful detection of the maser depends primarily on the distance to the star.

4.2 R Aquarii

The changes in intensity and velocity structure of the R Aqr maser between our 1987 (Paper I) and 1988 observations are no more extreme than variations noted in other SiO masers. For example, the previously cited investigation by Nyman & Olofsson (1986) revealed good correlation between optical and SiO maser ($v=1$, $J=2-1$) intensity. Large cycle-to-cycle variations in maximum intensity and velocity profiles were also apparent for many SiO sources. In the case of R Aqr (period ~ 387 d), the optical phase was almost the same during both our observing sessions: 0.91 in 1987 and 0.93 in 1988. Assuming the luminosity of the symbiotic maser to be determined only by the Mira phase, our data therefore suggest a slightly larger integrated intensity maximum for the 1988 cycle.

Recent *VLBI* studies (at 20 milliarcsec resolution) of the Mira variable R Cas (McIntosh *et al.* 1989) show that the distribution of SiO masers around that star is not uniform. Rather, the circumstellar environment appears clumpy, with maser emission from individual regions having well-defined velocity and polarization characteristics. The same investigation shows that single-antenna measurements reflect accurately the polarization state of at least some masing regions. Single-dish polarization data, although affected by spatial averaging, are therefore often useful in identifying radiation from individual clumps of maser activity. The most recent published 43 GHz interferometric observations of R Aqr (Hollis *et al.* 1986) have insufficient angular resolution to confirm a similarly clumpy dust shell. Pending further high-resolution *VLBI* studies, however, it is reasonable to assume that clumpiness is a feature of all SiO masers.

Barvainis & Predmore (1985) examined time variability in the polarization characteristics of seven SiO masers. They were unable to deduce any general trend from source to source, but noted that in some masers the position angle of certain profile features remained constant in the face of large changes in total or polarized fluxes. This is apparently the case with R Aqr. On the assumption that individual SiO maser profile features are due to radiation from spatially discrete sources, polarimetry may therefore afford a means of following the evolution of individual regions.

The radius of the long-period variable in the symbiotic system is likely to be $\sim 3\times10^{11}$ m and the maximum equatorial velocity ~ 10 km s^{-1} (Allen 1973 and references therein), giving a minimum rotation period of ~ 6 yr. Sreenivasan & Wilson (1978) show that stars losing mass (and hence angular momentum) may eventually attain much longer periods. In all but the fastest rotation case, the 1 yr interval between our consecutive observations of R Aqr is considerably smaller than the rotation period of the giant star and its envelope. We may therefore expect that our viewing geometry of the stellar environment and magnetic field remained similar for the two observations.

By contrast, the outflow velocity of 10 km s^{-1} (Paper I) carries material through an SiO maser zone of scale size ~ 1 stellar radius in ~ 1 yr. Thus, if we attribute emission at a particular velocity to a particular region, the observed stability in position angle favours a polarization model driven by the magnetic field rather than one based on geometrical asymmetries in the masing regions (Western & Watson 1983, 1984). This contention will strengthen if future data indicate stable (or at least predictable) position angles. Although relatively large magnetic fields (~ 1 G) are required to explain high fractional polarizations, observations of circular polarization in SiO maser emission (Barvainis, McIntosh & Predmore 1987) indicate that such fields do exist near some stars.

In Fig. 3(b) there is some tendency for stronger features to be the most weakly polarized. McIntosh *et al.* (1989) suggest that this commonly observed characteristic of SiO masers may be due either to Faraday depolarization along longer gain paths, or to blending of radiation from less uniform physical regions. The similarity between the 1988 R Aqr position angle profile (Fig. 3a) and the GL5552 profile (Fig. 2) is striking, although the PA swing is smaller in the case of R Aqr. The form of the profile is not encountered particularly frequently in other sources and the similarity may be coincidental. Nevertheless, it is possible to conceive of common magnetic field configurations or mass-loss geometries which could produce the observed profiles.

5 CONCLUSION

We are now able to define rules which virtually guarantee the presence of a detectable stellar SiO maser. These are: strong flux at a wavelength about 8–12 μm, e.g. *IRAS* flux; characteristics which do not result in exclusion on the basis of criteria (i)–(vi) given in Section 1, and optical variability in excess of 2.5 mag. Use of these rules should allow a further significant increase in the number of SiO masers available for study.

There is a clear need for a comprehensive southern

hemisphere study of mass loss from evolved stars, perhaps along the lines of the northern 2.6 mm CO survey by Knapp & Morris (1985). Complementary observational programmes which examine SiO maser sources for H_2O and OH emission may also be valuable, since a distance-independent estimate of mass-loss rate may be obtained by examining the intensity ratios of the various maser lines (see, for example, Bowers 1985). Whatever strategy is adopted, the resulting mass-loss data would be invaluable in verifying the proposed link between SiO maser emission and stellar mass-loss rate. If the link is confirmed, measurement of the time-averaged ratio of maser luminosity to IR flux could provide a convenient means of estimating mass-loss rate in stars having associated SiO masers.

Many objects selected on the basis of their *IRAS* colours are not identified with optical objects, and, indeed, some probably lack optical counterparts due to extreme circumstellar or interstellar reddening. We suggest that those extreme OH/IR stars (see, for example, Jones, Hyland & Gatley 1983; Jones *et al.* 1983) which have associated SiO masers are probably large-amplitude Mira variables. Of the 17 new masers which lack optical counterparts (those in Table 1 with IRC, OH, IRAS and GL designations), the *IRAS* catalogue gives 11 at least a 50 per cent chance of being variable, despite the scant temporal sampling by the satellite.

Finally, we note that most of the objects listed in Table 1 lack previously published radial-velocity values. Although SiO maser emission is not fully symmetric with respect to stellar velocity, the emission profiles shown in Fig. 1 undoubtedly provide a useful velocity guide to those who pursue kinematical studies of the evolved stellar population.

ACKNOWLEDGMENTS

We are grateful to Dr Jessica Chapman for useful comments on several aspects of the work presented in this paper. We thank H. Fagg and M. Smith for undertaking the exacting repair work necessary to re-commission the Parkes 43 GHz receiver after failure of the cryogenics system. Their efforts in installing and maintaining the receiver were also much appreciated. This work was supported in part by a joint CSIRO–University of Sydney grant.

REFERENCES

Allen, C. W., 1973. *Astrophysical Quantities,* 3rd edition, Chs 10 & 11, Athlone Press, London.

Allen, D. A., Hall, P. J., Norris, R. P., Troup, E. R., Wark, R. M. & Wright, A. E., 1989. *Mon. Not. R. astr. Soc.,* **236,** 363.

Balister, M., Batchelor, R. A., Haynes, R. F., Knowles, S. H., McCulloch, M. G., Robinson, B. J., Wellington, K. J. & Yabsley, D. E., 1977. *Mon. Not. R. astr. Soc.,* **180,** 415.

Barvainis, R. & Predmore, C. R., 1985. *Astrophys. J.,* **288,** 694.

Barvainis, R., McIntosh, G. C. & Predmore, C. R., 1987. *Nature,* **329,** 613.

Bowers, P. F., 1985. In: *Mass Loss From Red Giants,* p. 189, eds Morris, M. & Zuckerman, B., Reidel, Dordrecht.

Bujarrabal, V., Planesas, P. & del Romero, A., 1987. *Astr. Astrophys.,* **175,** 164.

Dickinson, D. F., Snyder, L. E., Brown, L. W. & Buhl, D., 1978. *Astr. J.,* **83,** 36.

Gehrz, R. D. & Woolf, N. J., 1971. *Astrophys. J.,* **165,** 285.

Haikala, L., 1989. In: *The Physics and Chemistry of Interstellar Molecular Clouds,* p. 136, eds Winnewisser, G. & Armstrong, J. T., Springer-Verlag, Berlin.

Hall, P. J., Wark, R. M. & Wright, A. E., 1987. *Proc. astr. Soc. Aust.,* **7,** 50.

Hollis, J. M., Michalitsianos, A. G., Kafatos, M., Wright, M. C. H. & Welch, W. J., 1986. *Astrophys. J.,* **309,** L53.

IRAS Science Team, 1986. *Astr. Astrophys. Suppl.,* **65,** 607.

Jones, T. J., Hyland, A. R. & Gatley, I., 1983. *Astrophys. J.,* **273,** 660.

Jones, T. J., Hyland, A. R., Wood, P. R. & Gatley, I., 1983. *Astrophys. J.,* **273,** 669.

Kholopov, P. N. (ed.), 1985. *General Catalogue of Variable Stars,* 4th edn, NAUKA, Moscow.

Knapp, G. R. & Morris, M., 1985. *Astrophys. J.,* **292,** 640.

McIntosh, G. C., Predmore, C. R., Moran, J. M., Greenhill, L. J., Rogers, A. E. E. & Barvainis, R., 1989. *Astrophys. J.,* **337,** 934.

Meadows, P. J., Good, A. R. & Wolstencroft, R. D., 1987. *Mon. Not. R. astr. Soc.,* **225,** 43P.

Merrill, K. M & Stein, W. A., 1986. *Publs astr. Soc. Pacif.,* **88,** 874.

Nyman, L.-A. & Olofsson, H., 1986. *Astr. Astrophys.,* **158,** 67.

Sivagnanam, P., Le Squeren, A. M., Foy, F. & Tran Minh, F., 1989. *Astr. Astrophys.,* **211,** 341.

Sreenivasan, S. R. & Wilson, W. J. F., 1978. *Astr. Astrophys.,* **70,** 755.

Wardle, J. F. C. & Kronberg, P. P., 1974. *Astrophys. J.,* **194,** 249.

Western, L. R. & Watson, W. D., 1983. *Astrophys. J.,* **268,** 849.

Western, L. R. & Watson, W. D., 1984. *Astrophys. J.,* **285,** 158.

Willems, F. J. & de Jong, T., 1986. *Astrophys. J.,* **309,** L39.